STUDY OF VARIOUS QUASI-LAGRANGIAN TECHNIQUES FOR NUMERICAL MODELS

J. Coiffier, P. Chapelet, N. Marie
Direction de la Météorologie Nationale
Paris, France

Summary: We study here the effect of various quasi-lagrangian techniques applied to the primitive equations. The impact of the time integration schemes is examined by calculating phase velocities of the propagating waves which are solutions of the linear equations. A shallow water model is used to study the behaviour of the slow moving wave while a baroclinic two-dimensional model gives knowledge of the gravity wave propagation properties as well as induced modifications to stationary flows forced by orography.

1. INTRODUCTION

A few years ago, severals attempts were made to build stable time integration schemes for numerical prediction models permitting a large time-step. A. J. Robert (1981) proposed to use the quasi-lagrangian technique for the treatment of the advective part of the equations which allows an increase of time-step without damaging model performances. Several variants of this method have been proposed (Bates, 1985; Ritchie, 1986).

We examine here the precision as well as the stability of the various proposed methods by comparing the results given by the numerical schemes with the analytical ones in the framework of linearised versions of the primitive equation models. In this presentation, care is taken to distinguish the effects of the time discretisation from those of the space discretisation and space interpolation. The shallow water models permit to study the behaviour of the slow moving waves while the two-dimensional baroclinic models are used to study how the speed of the gravity waves is modified and the consequenses of various discretisations on stationary flows forced by orography.

2. THE VARIOUS QUASI-LAGRANGIAN SCHEMES

Only schemes using centered time-differences have been examined. We suppose that we are able to determine with some accuracy the point where a particle is coming from.

The general form of the evolution equation for a given parameter X(x,y,t) can be written:

$$\frac{\partial X}{\partial t} + U \frac{\partial X}{\partial x} + V \frac{\partial X}{\partial y} = L.X + N(X) \cdot$$

L represents the linear part of the equations and N the residual non-linear part. The left hand side of the above equation is the expression of the lagrangian total derivative:

$$\frac{\partial X}{\partial t} + U \frac{\partial X}{\partial x} + V \frac{\partial X}{\partial y} \equiv \frac{dX}{dt} \quad .$$

2.1 Method with interpolation (Robert, 1982)

The evolution equation is discretised as follows:

$$\frac{X_G^{t+\Delta t} - X_O^{t-\Delta t}}{2\Delta t} = L. \frac{X_G^{t+\Delta t} + X_O^{t-\Delta t}}{2} + \left[N(X^t)\right]_I \quad ,$$

X_G is the value of X at grid point G (see Fig.1a),

X_O is the value of X at the point O where the particle comes from,

X_I is the value of X at the mid-point I between O and G.

Superscripts t, $t-\Delta t$, $t+\Delta t$, refer to time levels.
This methods needs the interpolation of $X^{t-\Delta t}$ at point O and $N(X^t)$ at point I, (Figure 1a).

2.2 Method avoiding one interpolation (Ritchie, 1986)

We define the point O' as the closest grid point to O and I' the mid-point between O' and G (Figure 1b). We can write:

$$U = U^* + U' \qquad V = V^* + V'$$

where $2\Delta t U^*$ and $2\Delta t V^*$ are the components of the vector $\overrightarrow{O'G}$.
The method consists in a lagrangian treatment of the advection by the wind (U^*, V^*), the remaining advection by the residual (U', V') being incorporated into the non linear part which appears in the right hand side. This discretisation reads:

$$\frac{X_G^{t+\Delta t} - X_{O'}^{t-\Delta t}}{2\Delta t} = L. \frac{X_G^{t+\Delta t} + X_{O'}^{t-\Delta t}}{2} + \left[N(X^t)\right]_{I'} - \left(U'\frac{\partial X}{dx} + V'\frac{\partial X}{\partial y}\right)^t_{I'}.$$

This method avoids the interpolation at point O and the residual interpolation at the point I' is very simple due to the three possible locations (Figure 1c).

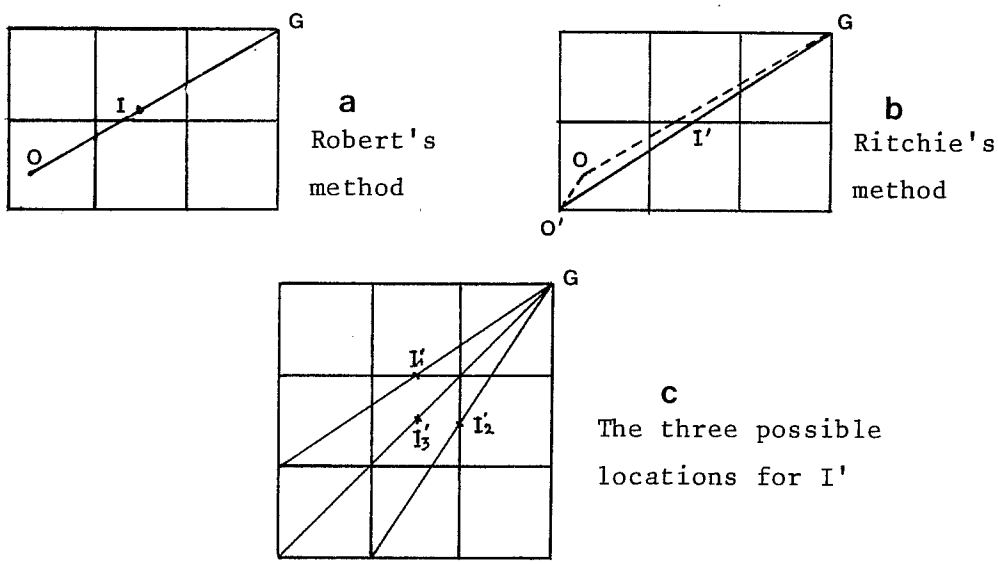

Figure 1. Location of the points where the interpolation is performed for quasi-lagrangian techniques.

2.3 Method without any interpolation (Geleyn, 1986)

One supplementary simplification can be achieved by evaluating the remaining non linear terms by taking the average at time t between their values at grid points G and O':

$$\left[N(X^t)\right]_{I'} - \left(U'\frac{\partial X}{\partial x} + V'\frac{\partial X}{\partial y}\right)^t_I = \frac{1}{2}\left\{\left[N(X^t)\right]_G + \left[N(X^t)\right]_{O'} - \left[\left(U'\frac{\partial X}{\partial x} + V'\frac{\partial X}{\partial y}\right)^t_G + \left(U'\frac{\partial X}{\partial x} + V'\frac{\partial X}{\partial y}\right)^t_{O'}\right]\right\}.$$

3. LINEARISED SHALLOW WATER MODELS

In order to study the accuracy and the stability of various time-integration schemes, we compute the solutions of the corresponding models, which can then be compared with the analytical solution.

3.1 Equations

We assume a geostrophic mean flow characterised by $\bar{U}$, $\bar{V}$ and $\bar{\Phi}(x,y)$ and a topography $\bar{\Phi}_s(x,y)$ parallel to the free surface $\bar{\Phi}(x,y)$. We make the f-plane approximation and call $\bar{\Phi}_o$ the mean value of the geopotential thickness $(\bar{\Phi}-\bar{\Phi}_s)$. With these assumptions the linearised equations for the perturbations U, V and Φ have the following form:

$$\frac{\partial U}{\partial t} + \bar{U}\frac{\partial U}{\partial x} + \bar{V}\frac{\partial U}{\partial y} - f.V + \frac{\partial \Phi}{\partial x} = 0$$

$$\frac{\partial V}{\partial t} + \bar{U}\frac{\partial V}{\partial x} + \bar{V}\frac{\partial V}{\partial y} + f.U + \frac{\partial \Phi}{\partial y} = 0$$

$$\frac{\partial \Phi}{\partial t} + \bar{U}\frac{\partial \Phi}{\partial x} + \bar{V}\frac{\partial \Phi}{\partial y} + \Phi_0\left(\frac{\partial U}{\partial x} + \frac{\partial V}{\partial y}\right) = 0 \quad .$$

3.2 Analytical solutions

Assuming periodic boundary conditions we want to determine wave propagating solutions of the form:

$$X = X^* e^{i(kx+ly+\omega t)},$$

k and l being the wave numbers along x and y axis and ω the frequency. The solutions can be obtained by solving the homogeneous system:

$$\begin{pmatrix} i(\omega+k\bar{U}+l\bar{V}) & -f & ik \\ +f & i(\omega+k\bar{U}+l\bar{V}) & il \\ i\bar{\Phi}_o & i\bar{\Phi}_o & i(\omega+k\bar{U}+l\bar{V}) \end{pmatrix} \times \begin{pmatrix} U \\ V \\ \Phi \end{pmatrix} = 0 \quad .$$

Non-trivial solutions are obtained when the determinant of the matrix is zero. Calling μ the quantity $\omega + k\bar{U} + l\bar{V}$, the condition leads to the third degree equation:

$$\mu \left\{ \mu^2 - \left[f^2 + \bar{\Phi}_o(k^2+l^2) \right] \right\} = 0 \quad .$$

We have three solutions for μ and thus for ω :
$\omega_1 = -(k\bar{U}+l\bar{V})$: the slow solution,
$\omega_{2,3} = -(k\bar{U}+l\bar{V}) \pm \left[f^2 + \bar{\Phi}_o(k^2+l^2) \right]^{1/2}$: these are the two fast moving inertia-gravity solutions.

3.3 Effect of the space discretisation

The effect of replacing space derivatives by finite differences on a grid modifies the preceding results. Making the traditional discretisation on a "Arakawa-C" grid leads to the introduction of wave depending damping factors:

$$S_2 = \frac{\sin(k\Delta x)}{k\Delta x} \quad \text{and} \quad T_2 = \frac{\sin(l\Delta x)}{l\Delta x} \quad \text{in front of the advective terms,}$$

$$S_3 = \frac{\sin(k\Delta x/2)}{k\Delta x/2} \quad \text{and} \quad T_3 = \frac{\sin(l\Delta x/2)}{l\Delta x/2} \quad \text{in front of the adaptative terms,}$$

and $Q_3 = S_3T_3$ in front of the Coriolis terms.

The third degree equation becomes:

$$\mu \left\{ \mu^2 - \left[Q_3^2 f^2 + \bar{\Phi}_o(S_3^2k^2+T_3^2l^2) \right] \right\} = 0$$

with: $\mu = \omega + S_2k\bar{U} + S_3l\bar{V}$,

which finally gives for ω :

$$\omega_1 = -(S_2 k\bar{U} + T_2 l\bar{V})$$
$$\omega_{2,3} = -(S_2 k\bar{U} + T_2 l\bar{V}) \pm \left[Q_3^2 f^2 + \Phi_o (S_3^2 k^2 + T_3^2 l^2) \right]^{1/2} .$$

The effect of the spatial discretisation on the grid is a decrease of the effective phase velocity of the waves. The larger the wave numbers k and l the more important this effect. This is a well known result and in order to simplify further we shall suppose hereafter that spatial derivatives are exactly evaluated, (by means of the spectral method for example).

3.4 Centered explicit model

The time derivative of X is evaluated by time centered differences:

$$\frac{\partial X}{\partial t} \simeq \frac{X^{t+\Delta t} - X^{t-\Delta t}}{2\Delta t} .$$

Assuming the same form as before for X, this discretisation leads to replace $i\omega$ by $iS_1\omega$ with:

$$S_1 = \frac{\sin(\omega\Delta t)}{\omega\Delta t} .$$

The solutions read in this case:

$$\sin(\omega\Delta t) = -(k\bar{U}+l\bar{V})\,\Delta t$$
$$\sin(\omega\Delta t) = \left\{ -(k\bar{U}+l\bar{V}) \pm \left[f^2 + \Phi_o (k^2+l^2) \right]^{1/2} \right\} \Delta t .$$

This scheme will be stable if the frequencies ω are real (i.e. the right hand sides must be between -1 and +1).

This leads to the criterion:

$$\left\{ (k\bar{U}+l\bar{V}) \pm \left[f^2 + \Phi_o (k^2+l^2) \right]^{1/2} \right\}^2 \Delta t^2 \leq 1 .$$

We obtain in total six solutions because there are two solutions for the arcsin function. Retaining only the three solutions corresponding to the physical modes gives:

$$\omega_1 = \frac{1}{\Delta t} \arcsin \left[-\left(k\bar{U}+l\bar{V} \right) \Delta t \right] .$$

$$\omega_{2,3} = \frac{1}{\Delta t} \arcsin\left[\left\{-\left(k\bar{U}+l\bar{V}\right) \mp \left[f^2 + \Phi_0 (k^2+l^2)\right]^{1/2}\right\} \Delta t\right] .$$

3.5. Centered semi-implicit scheme

The time derivative is calculated as before while the adaptation terms are averaged between time levels $t - \Delta t$ and $t + \Delta t$:

$$\bar{X}^{2t} = \frac{1}{2} (X^{t+\Delta t} + X^{t-\Delta t}) .$$

This procedure introduces a factor $C_1 = \cos(\omega \Delta t)$ in front of the adaptation terms and gives:

$$\omega_1 = \frac{1}{\Delta t} \arcsin\left[-\left(k\bar{U}+l\bar{V}\right)\Delta t\right] .$$

$\omega_{2,3}$ are obtained by solving a second degree equation for $\sin(\omega \Delta t)$:

$$\left[\sin(\omega\Delta t)+\left(k\bar{U}+l\bar{V}\right)\Delta t\right]^2 = \left\{f^2 + \Phi_0 \left[1-\sin^2(\omega\Delta t)\right] [k^2 + l^2]\right\} \Delta t^2 .$$

The slow solution is identical to the explicit one and gives the stability criterion:

$$(k\bar{U} + l\bar{V})^2 \Delta t^2 \leqslant 1. .$$

3.6 Quasi-lagrangian semi-implicit scheme (Robert, 1981)

By assuming that the interpolation at the point O where the particle comes from is exactly evaluated, the discretisation of the total derivative dX/dt by $(X^{t+\Delta t} - X^{t-\Delta t})/2\Delta t$ gives:

$$\frac{X^{t+\Delta t} - X_o^{t-\Delta t}}{2\Delta t} = i \frac{S_1'}{\Delta t} X_I ,$$

(the subscript I refers here to the mid-point value) with $S_1' = \sin\left[(\omega + k\bar{U} + l\bar{V}) \Delta t\right]$.

Similarly adaptative terms are computed by taking the average:

$$\bar{X}^{2t} = \frac{X^{t+\Delta t} + X_o^{t-\Delta t}}{2} = C_1' X_I ,$$

with $C_1' = \cos\left[(\omega + kU + lV) \Delta t\right]$.

Solving the corresponding characteristic equation gives for the physical solutions:

$$\omega_1 = -\left(k\bar{U}+l\bar{V}\right) \quad ,$$

$$\omega_{2,3} = -\left(k\bar{U}+l\bar{V}\right) \mp \frac{1}{\Delta t} \operatorname{arctg} \left\{ \Delta t \left[\frac{f^2 + \Phi_0 (k^2 + l^2)}{1 - \Delta t^2 f^2} \right]^{1/2} \right\} \quad ,$$

with the stability criterion: $f^2 \Delta t^2 < 1$.

We can also take into account the effect of the interpolation. In the case of the linear interpolation and for the restricted one-dimensional case ($l = 0$) we get a complex value $\omega_r + i\omega_i$ for the solutions. This indicates that the amplitude is no longer conserved. We obtain for the slow solution:

$$\omega_{r_1} = \frac{1}{\Delta t} \left\{ \frac{kp\Delta x}{2} + \frac{1}{2} \operatorname{arctg} \frac{\delta \sin(k\Delta x)}{1-\delta[1-\cos(k\Delta x)]} \right\} \quad ,$$

where p is the grid point verifying:

$$(p+1)\Delta x \leqslant 2\bar{U}\,\Delta t < p\,\Delta x$$

and δ the normalised distance $p - 2\bar{U}\,\Delta t/\Delta x$.

The amplification factor ρ is given by:

$$|\rho^4| = 1 - 2\delta(1-\delta)[1 - \cos(k\,\Delta x)] .$$

This expression means that $|\rho|^4 \leqslant 1$ (stable scheme) provided $0 \leqslant \delta \leqslant 1$. The interpolation must be done by using the grid point values around the origin point (Bates, 1985).

3.7 Scheme avoiding the interpolation (Ritchie, 1985)

Following Ritchie's method the lagrangian derivative is calculated between points O' and G, where O' is the closest point to O where the particle comes from. The components of the distance O'G are $p\,\Delta x$, $q\,\Delta x$ and in this case we obtain for the slow solution:

$$\omega_1 = -\frac{1}{\Delta t}\left(\frac{kp\Delta x}{2} + \frac{lq\Delta x}{2}\right) - \frac{1}{\Delta t} \arcsin\,[(kU'+lV')\Delta t] \quad ,$$

$\omega_{2,3}$ are obtained from the solutions of the second degree equation for the quantity:

$$S_1'' = \sin\left(\omega\Delta t + kp\frac{\Delta x}{2} + lq\frac{\Delta x}{2}\right) \quad :$$

$$[S_1'' + (kU'+lV')\Delta t]^2 = \left[f^2 + \Phi_0 \left(1 - S_1''^2\right) (k^2 + l^2) \right] \Delta t^2 \ .$$

The stability criterion is now given by:

$$(kU' + lV')^2 \Delta t^2 \leqslant 1,$$

which is analogous to that we obtained with the semi-implicit scheme, replacing $(\bar{U}, \bar{V})$ by the residual velocity (U', V').

3.8 The scheme without any interpolation (Geleyn, 1986)

If the residual advective and Coriolis terms are evaluated at time t by averaging their values at the departure point and at the arriving point, we obtain a solution analogous to the preceding one, where the terms $(kU'+lV') \cdot \Delta t$ and f are multiplied by the attenuation factor $C = \cos(lp\,\Delta x/2 + lq\,\Delta x/2)$.

3.9 Behaviour of the slow moving wave

If we are interested in the behaviour of the slow moving wave, we can evaluate the efficiency of the scheme by calculating the ratio $r = \omega_{numerical}/\omega_{analytical}$ for several values of the number $\kappa = 2\bar{U}\Delta t/\Delta x$ (restricting now our comparison to the one-dimensional case).

The results are displayed in figures 2a, 2b, 2c for various values of the wavelength λ. In this comparison only the effect of the time discretisation has been taken into account. For the classical quasi-lagrangian method we just assumed a linear interpolation at the origin point.

We remark that the quasi-lagrangian scheme (dashed line) gives a high precision if sufficiently large values of the wavelength and κ are considered.

The method proposed by Ritchie (dash-dotted line), which coincides with the conventional semi-implicit one for $\kappa < 0.5$ looks like the Robert method for large values of the number κ. The method proposed by Geleyn in order to avoid any interpolation is not as precise as the preceding ones for small wavelengths but becomes acceptable for wavelengths larger than $16\Delta x$.

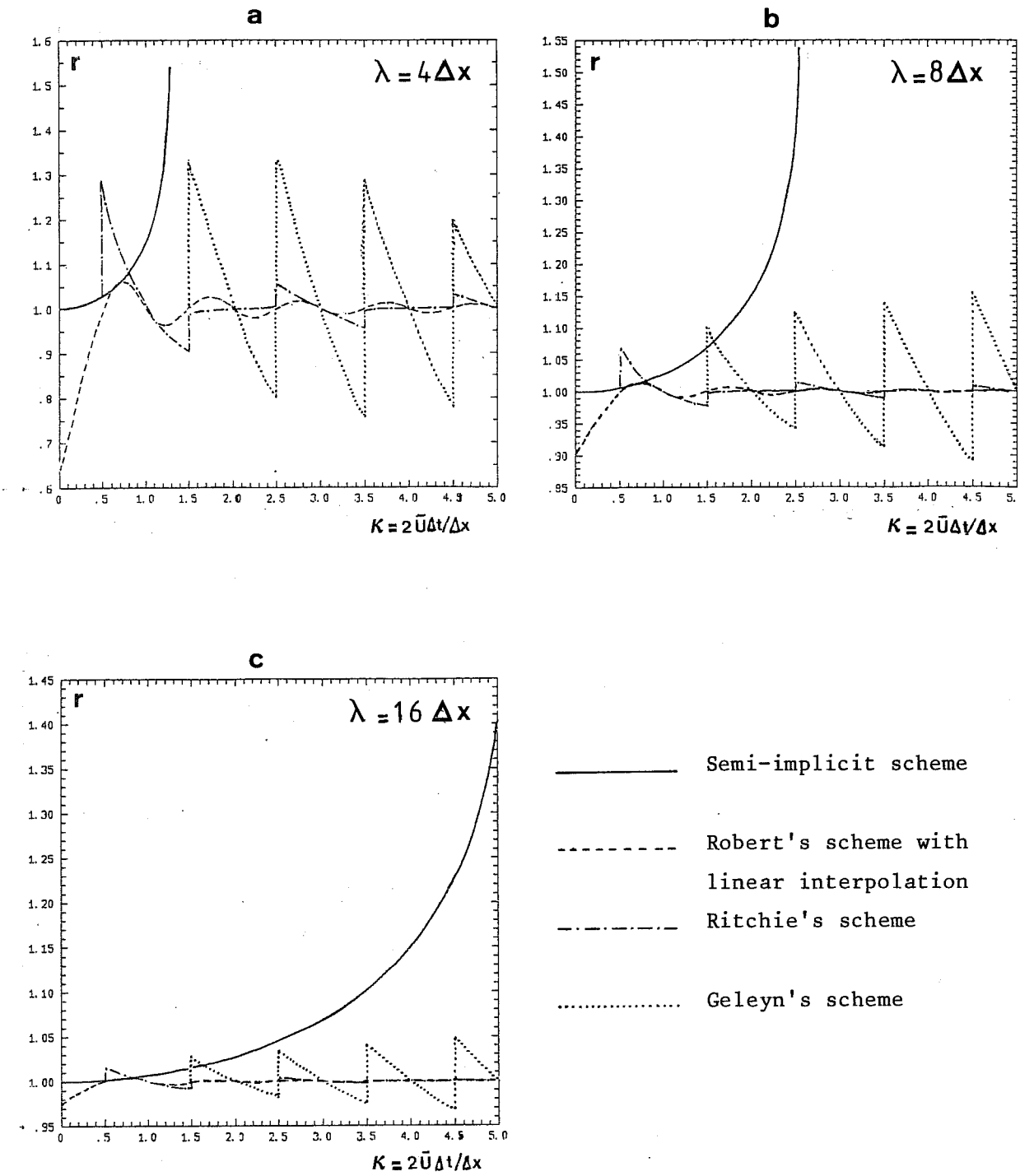

Figure 2. Effect of the time integration on the slow wave for various values of the wavelength.

4. NUMERICAL EXPERIMENTATION WITH THE NON LINEAR MODEL

4.1 Limited area experimental framework.

Several tests have been carried out with the non linear barotropic model using the grid of the PERIDOT model: "Arakawa-C", 51x51 points, 38.1 km (Imbard et al., 1986). Initial values as well as boundary values were calculated from 500 hPa analyses every 6 hours on a larger domain (63X63 points) in order to be able to achieve the interpolation at the origin point. We used a reduced geopotential variable $\Phi = (\Phi_{500hPa} - 40000)$ in order to have a reasonable mean divergence. The treatment of the boundary conditions was identical to that of the PERIDOT model. The weighting coefficients were calculated depending on the time step to keep the same value of the relaxation factor for a given grid point. The time-step was 4 min. for the semi-implicit integration and 20 min. for the quasi-lagrangian experiments. For the application of the quasi-lagrangian techniques the following interpolations were carried out:

- interpolation of the wind to determine the trajectories: bilinear,
- interpolation at points O and I: bicubic,
- interpolation at point I' (Ritchie's method): linear or bilinear.

4.2 Experimental results

The initial state (Figure 3) is characterised by a northerly flow over France associated with a low which is located in the northern part of Italy. After 48 hours a low coming from the north is located just over Paris while the italian low tends to disappear (Figure 4).

The examination of the forecasts given by the various methods leads to the following conclusions: all the methods give analogous results (Figures 5 to 8). The methods avoiding interpolation place the centre of the low over the Channel while the right position is rather the Seine basin (Figures 7 and 8). We also remark that the method without interpolation produces some noise particularly over the Mediteranean Sea. This effect can be due to threshold effects associated with the search for the closest grid point to the origin. It must also be mentioned that Geleyn's method (without any interpolation, figure 8) gives the same result as Ritchie's one.

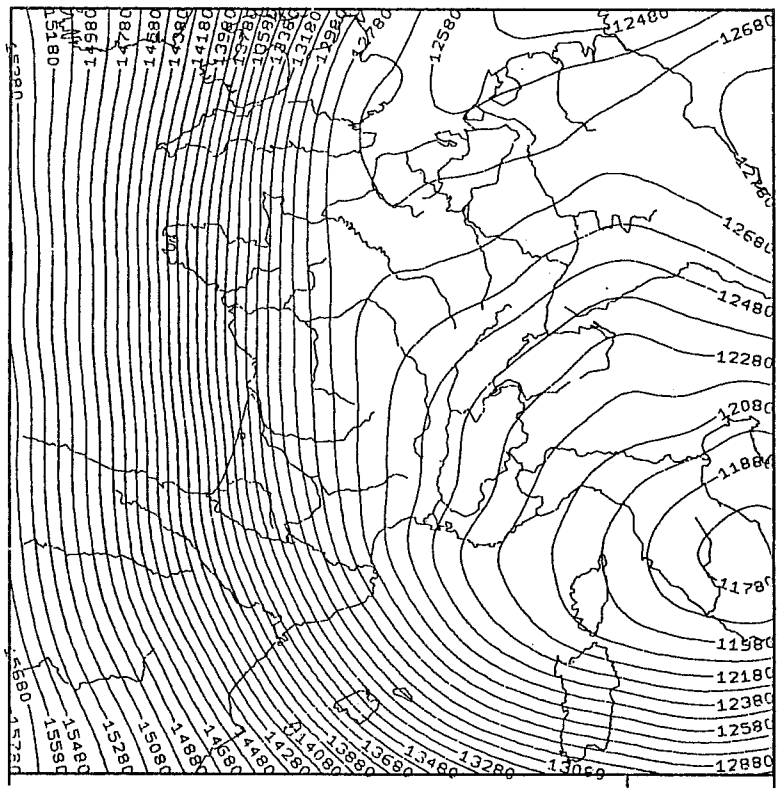

Figure 3. Analysis for 18-03-85 at 00 GMT

Reduced geopotential (J/kg)

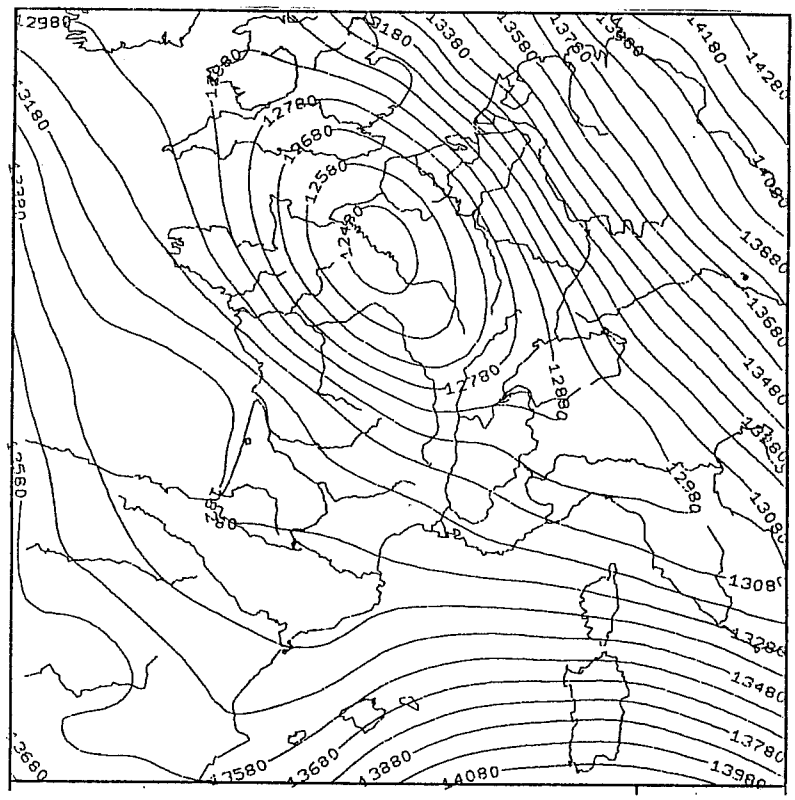

Figure 4. Analysis for 20-03-85 at 00 GMT

Reduced geopotential (J/kg)

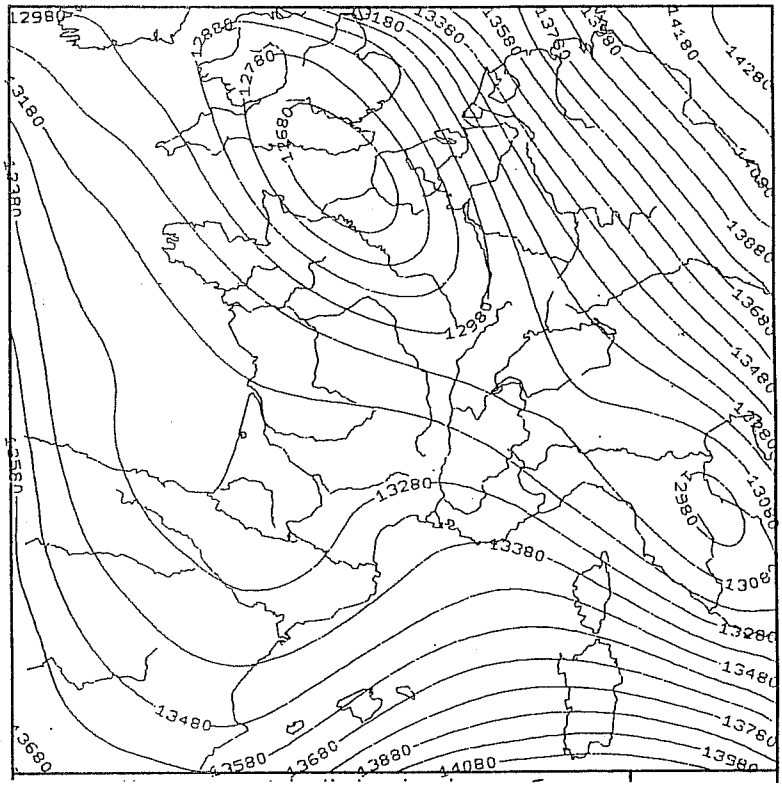

Figure 5. 48 h. forecast, Semi-implicit scheme
Reduced geopotential (J/kg)

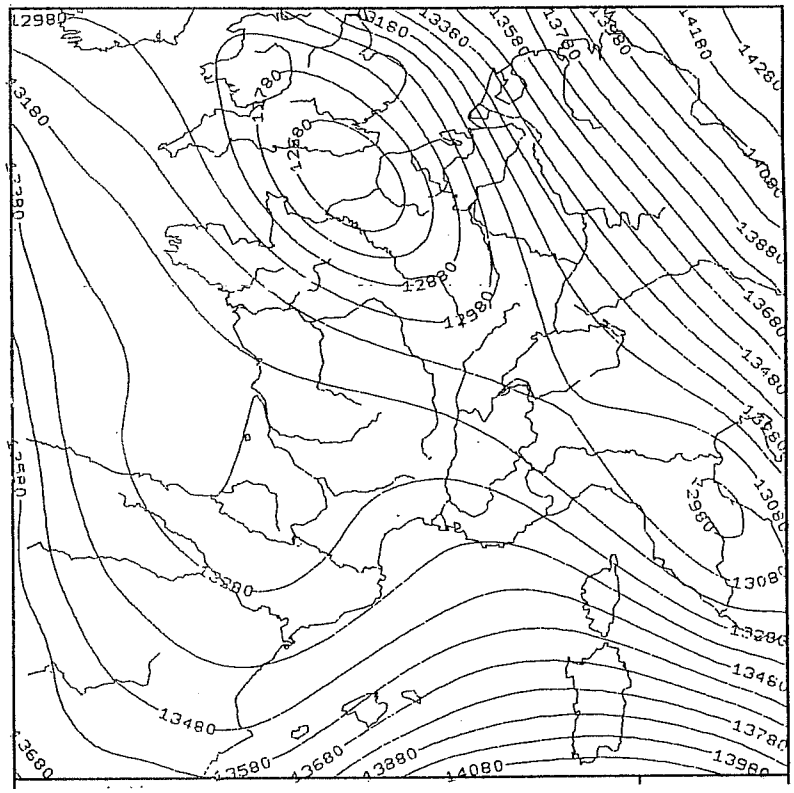

Figure 6. As fig. 5 except for Robert's scheme

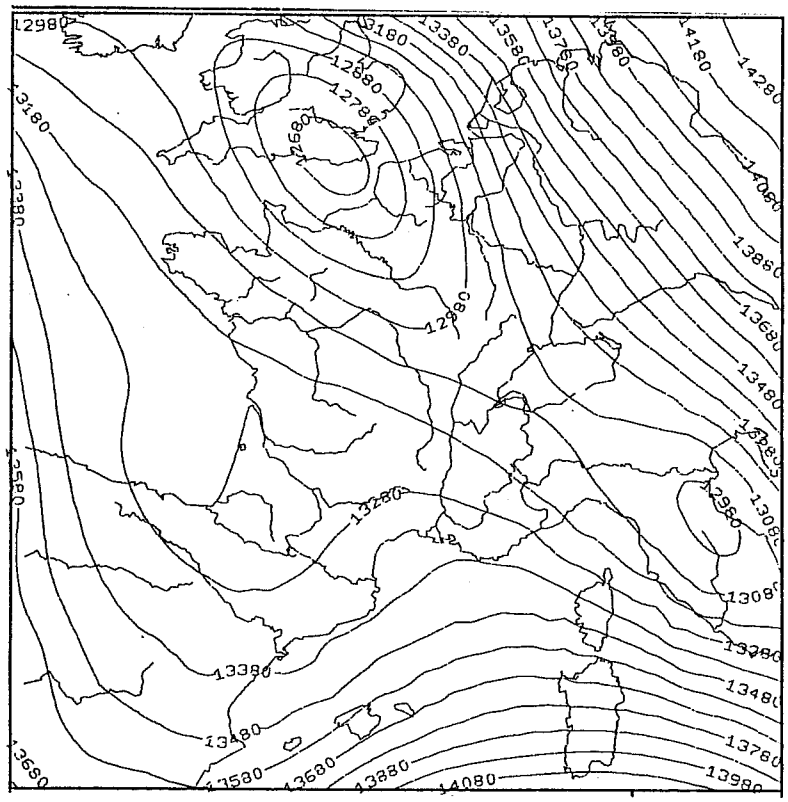

Figure 7. As fig. 5 except for Ritchie's scheme

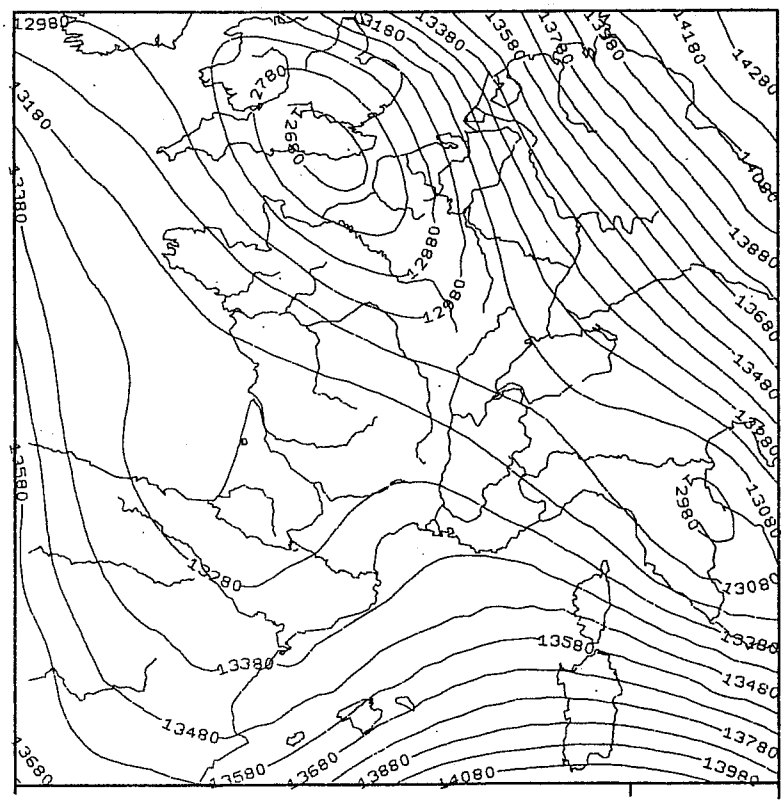

Figure 8. As fig. 5 except for Geleyn's scheme

5. THE TWO-DIMENSIONAL LINEARISED BAROCLINIC MODEL

5.1 Equations

We study a two-dimensional baroclinic flow and linearise the primitive equations. As a vertical coordinate we use the hybrid vertical coordinate s. We assume a basic state characterised by $\bar{p}_s$ (fixed surface pressure), $\bar{T}$ (isothermal temperature profile) and $\bar{U}$ (constant horizontal wind velocity). The linearised set of equations for the perturbations U, T, p_s can now be written as:

$$\frac{\partial U}{\partial t} = -\bar{U}\frac{\partial U}{\partial x} - B\frac{\partial T}{\partial x} - G\frac{\partial p_s}{\partial x}$$

$$\frac{\partial T}{\partial t} = -\bar{U}\frac{\partial T}{\partial x} - A\frac{\partial U}{\partial x}$$

$$\frac{\partial p_s}{\partial t} = -\bar{U}\frac{\partial p_s}{\partial x} - S'\frac{\partial U}{\partial x} \quad .$$

U and T are N element column vectors corresponding to the values of the perturbations for the N levels of the model.

B is a NxN matrix which characterises the discretisation of the linear part of the hydrostatic equation.

A is a NxN matrix which corresponds to the discretised expression of the energy conversion term.

G is a column vector corresponding to the discretisation of the term $(RT/C_pp)\partial p/\partial p_s$.

S' is a row vector whose elements are the layer thicknesses for the reference value $\bar{p}_s$ of the surface pressure.

5.2 Analytical solutions

Assuming periodic boundary conditions, solutions of the form $X = X^*e^{ik(x-ct)}$ can be determined .

These are the solutions of the 2N+1 order homogeneous system:

$$\begin{bmatrix} \bar{U}-c & B & G \\ A & \bar{U}-c & 0 \\ S' & 0 & \bar{U}-c \end{bmatrix} \begin{pmatrix} U^* \\ V^* \\ \Phi^* \end{pmatrix} = 0 \quad .$$

Setting $\bar{U} - c = -\mu$ we obtain:

$$-\mu U^* + BT^* + Gp_s^* = 0$$
$$AU^* = \mu T^*$$
$$S'U^* = \mu p_s^* \quad .$$

(i) If $\mu = 0$ we get:

$$(M - \mu^2 I)U^* = 0 \text{ with } M = BA+GS' .$$

The μ^2 are the eigenvalues of the vertical stucture matrix M and we get 2N solutions given by:

$$c_i = \bar{U} \pm \mu_i , \qquad i=1,\ldots,N$$

corresponding to the eigenvectors:

U_i^*: eigenvector of the matrix M
$T_i^* = A\, U^*/\mu_i$
$p_{s_i}^* = S'U^*/\mu_i$.

(ii) if $\mu = 0$ then $c = \bar{U}$.
This is the slow solution with the associated eigenvector:

$U^* = 0$
$T^* = B^{-1}Gp_s$
p_s^* arbitrarily chosen.

The 2N+1 solutions are the normal modes of the linearised system.

5.3 Effect of the space discretisation

If we use a "Arakawa_C" grid, we have to introduce the S_2 and S_3 factors in front of the advective and adaptative terms respectively, as before in the barotropic case, after which the velocities become:

$$c_i = S_2\bar{U} \pm S_3\mu_i , \quad i=1,\ldots,N.$$

The eigenvectors are not modified.

5.4 Centered explicit model

The evaluation of the time derivatives by use of centered differences leads to replace $\partial X/\partial t$ by $S_1\partial X/\partial t$ which gives the relation:

$S_1 c_E = S_2\bar{U} \pm S_3\mu$ and then:

$$c_E = \frac{1}{k\Delta t}\arcsin\left[k\Delta t\left(S_2\bar{U} \mp S_3\mu\right)\right] \quad .$$

5.5 Semi-implicit model

The time averaging introduces a supplementary factor $C_1 = \cos(\omega\Delta t)$ in front of the adaptative terms and we have the relation:

$$S_1 c_{SI} = S_2 \pm C_1 S_3\mu \quad ,$$

which gives after solving a second degree equation for $\sin(\omega\Delta t)$:

$$c_{SI} = \frac{1}{k\Delta t}\arcsin\left\{\frac{S_2\bar{U} \mp \mu S_3\left[1+k^2\Delta t^2\left(\mu^2 S_3^2 - \bar{U}^2 S_2^2\right)\right]^{1/2}}{1 + S_3^2\mu^2 k^2\Delta t^2}\, k\Delta t\right\} \quad .$$

5.6 The quasi-lagrangian semi-implicit model

Keeping the same notations as before for the "origin" and "mid-point", the discretisation of the model reads:

$$\frac{X^{t+\Delta t} - X_o^{t-\Delta t}}{2\Delta t} = i\frac{\sin\left[\left(\omega+k\bar{U}\right)\Delta t\right]}{k\Delta t} \cdot kX_I^t = S'_1 . ikX_I^t \quad .$$

The adaptation terms are averaged so that:

$$\frac{X^{t+\Delta t} - X_o^{t-\Delta t}}{2} = \cos\left[\left(\omega+k\bar{U}\right)\Delta t\right] X_I^t = C'_1 . X_I^t \quad ,$$

which leads to the formula:

$$S'_1 = \pm C'_1 S_3\mu \quad ,$$

and the velocity becomes:

$$c_{QL} = \bar{U} \mp \frac{1}{k\Delta t}\operatorname{arctg}(k\Delta t S_3\mu) \quad .$$

The above calculations have been made by assuming that the values of x at points O and I are exactly interpolated. In the practical cases these values

have to be interpolated. We introduce the complex number γ_k as response of the interpolator for a periodic function of wave number k, so that $X_{interpolated} = \gamma_k \cdot X_{exact}$. The preceding results are modified as a consequense of the complex value of the wave velocity.

We obtain:

$$(c_{QL})_r = \bar{U} - \frac{1}{2k\Delta t} \mathrm{Arg}\,(\gamma_k) \mp \frac{1}{k\Delta t} \mathrm{arctg}(k\Delta t S_3 \mu)$$

$$(c_{QL})_i = - \frac{1}{2k\Delta t} \mathrm{Log}(\gamma_k) \quad .$$

The imaginary part of the velocity implies that the solution is damped, the damping factor being $\rho = |\gamma_k|^{1/2}$.

These general formulae allow us to determine the propagating properties for various interpolations.

Linear interpolation gives:

$$(c_{QL})_r = \frac{1}{2k\Delta t} \mathrm{arctg} \frac{\delta \sin(k\Delta x)}{1-\delta[1-\cos(k\Delta x)]} + \frac{p\Delta x}{2\Delta t} \mp \frac{1}{k\Delta t} \mathrm{arctg}(k\Delta t S_3 \mu)$$

$$\rho = \{1-2\delta(1-\delta)\,[1 - \cos(k\Delta x)]\}^{1/4} \quad ,$$

where p is so that: $p\Delta x > 2\bar{U}\Delta t \geq (p+1)\Delta x$
and $\delta = p - 2\bar{U}\Delta t/\Delta x$.

In the case of the cubic interpolation we find:

$$(c_{QL})_r = \bar{U} - \frac{1}{k\Delta t}\left\{\frac{1}{2}\mathrm{arctg}\left[\mathrm{tg}\frac{k\Delta x}{2}\,\frac{1+\frac{2}{3}\sin^2\frac{k\Delta x}{2}\delta(1-\delta)}{1+2\sin^2\frac{k\Delta x}{2}\delta(1-\delta)}(1-2\delta)\right] \mp \mathrm{arctg}(k\Delta t S_3 \mu)\right\}$$

$$\rho = \left\{\cos^2\frac{k\Delta x}{2}\left[1+2\sin^2\frac{k\Delta x}{2}\delta(1-\delta)\right]^2 + \sin^2\frac{k\Delta x}{2}\left[1+\frac{2}{3}\sin^2\frac{k\Delta x}{2}\delta(1-\delta)\right]^2(1-2\delta)^2\right\}^{1/4}.$$

5.7 Comparison between the various schemes

By comparing the results of the computed gravity wave velocities with the analytical ones, it appears that the time integration scheme modifies the propagating properties of these waves. In order to see more clearly the effect of the numerical schemes, we computed the values of $\mathcal{R} = c/\bar{U}$, the ratio of the numerical gravity wave velocity and the mean flow velocity

(similar to an inverse Froude number) and studied its variations with respect to the Courant number $k\bar{U}\Delta t$ for various values of the parameter $\tau = \mu/\bar{U}$.

The results are plotted on figures 9a, 9b and 9c, corresponding to the values $\tau = 5$, $\tau = 1$ and $\tau = .2$. Calculations have been made assuming an exact evaluation of the interpolated values at the origin point.

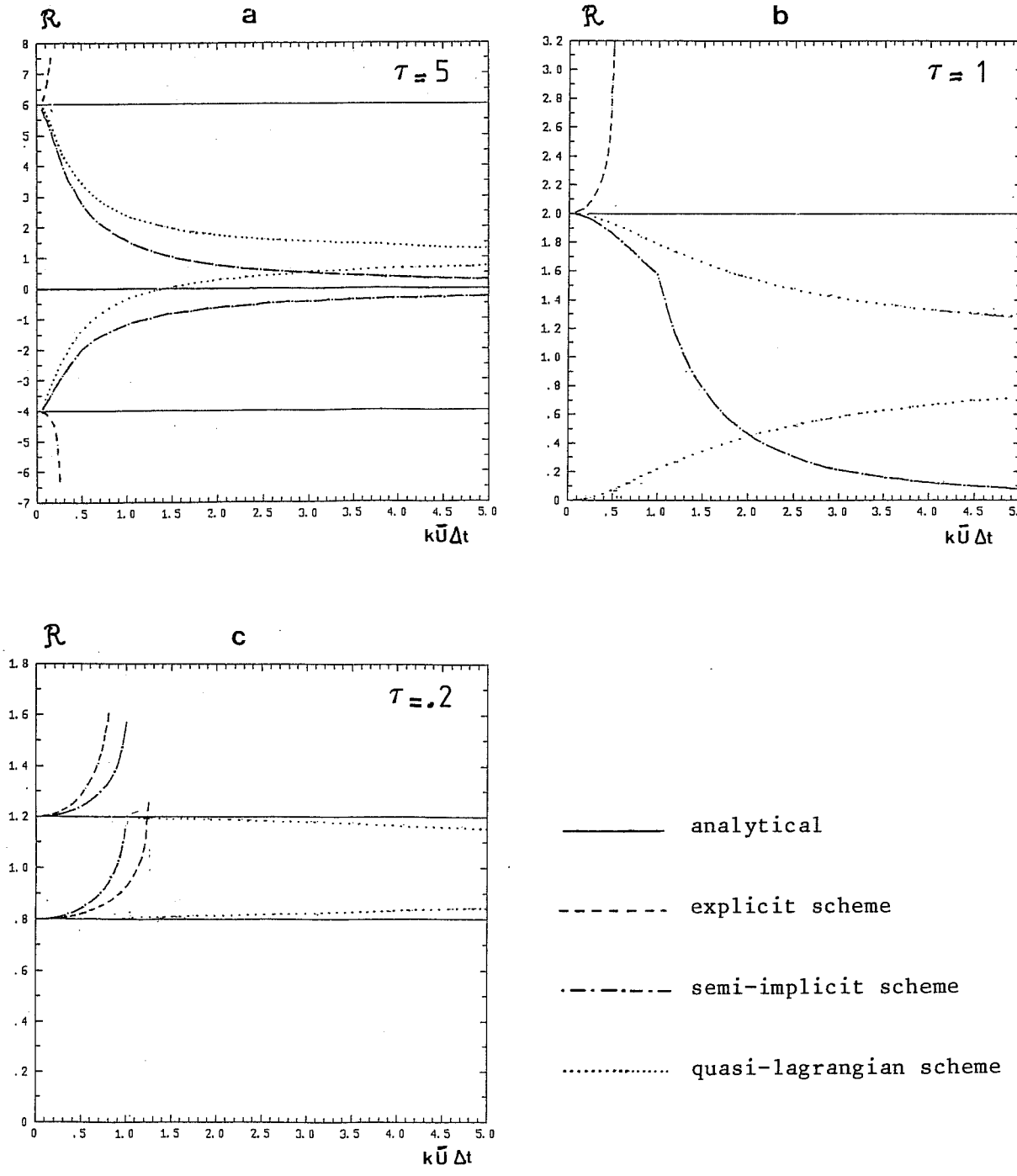

Figure 9. Effect of the time integration schemes on the gravity waves for various values of the ratio $\tau = \mu/\bar{U}$.

The figure 9a, which corresponds to the external gravity wave case, shows that the quasi-lagrangian scheme (dotted line) strongly modifies the speed of the gravity waves. The absolute value of the retrograde wave decreases and becomes zero when the Courant number reaches approximately 1.4. For this value there is a wave number which gives a stationary solution. When the Courant number is greater than this value the wave propagates in the wrong direction. Figure 9b corresponds to the critical case when one of the gravity waves is actually stationary. Here again the quasi-lagrangian scheme gives a prograde wave. The figure 9c shows that for internal waves the effect of the scheme is not as detrimental as for the other cases.

6. STATIONARY SOLUTIONS WITH OROGRAPHIC FORCING FOR THE LINEAR MODEL

6.1 Modified momentum equation

We now want to determine the response of the linear model to orographic forcing. We introduce for the uppermost layers of the model a dissipation term (horizontal diffusion term) in order to avoid the false reflection of the waves due to the unrealistic boundary condition at the top of the atmosphere (Klemp and Lilly, 1978). The momentum equation for instance reads:

$$\frac{\partial U}{\partial t} = -\bar{U}\frac{\partial U}{\partial x} - B\frac{\partial T}{\partial x} - G\frac{\partial p_s}{\partial x} \underbrace{- \frac{\partial \Phi_s}{\partial x}}_{\text{orographic term}} + \nu\frac{\partial^2 U}{\partial x^2} \quad ,$$

where Φ_s is the surface geopotential (depending only on the variable x) and ν is the viscous dissipation coefficient.

6.2 Analytical stationary solution

Fourier transformation of the modified equations gives the time evolution equations for the Fourier coefficients relative to the wave number k.

$$\frac{d\hat{U}_k}{dt} = -ik\bar{U}\,\hat{U}_k - ikB\,\hat{T}_k - ikG\,\hat{p}_{sk} - ik\,\hat{\Phi}_{sk} - k^2\nu\,\hat{U}_k$$

$$\frac{d\hat{T}_k}{dt} = -ik\bar{U}\,\hat{T}_k - ikA\,\hat{U}_k$$

$$\frac{d\hat{p}_{sk}}{dt} = -ik\bar{U}\,\hat{p}_{sk} - ikS'\hat{U}_k \quad .$$

The stationary solution is obtained by setting the time derivatives equal to zero. Then the elimination of $\hat{p}_{sk}$ and $\hat{T}_k$ in the above system leads to the relation:

$$\hat{U}_k = \left[M - \left(1 - \frac{ik\nu}{\bar{U}}\right) \bar{U}^2 \right]^{-1} \bar{U}\, \hat{\Phi}_{sk} \quad .$$

6.3 Stationary solution for the explicit or semi-implicit schemes

The discretisation on a "Arakawa_C" grid introduces the above mentioned factors S_2 and S_3 in the equations. The discretisation of the time derivatives as well as the averaging of the linear part of the equations has no influence on the result and the stationary solution becomes:

$$\hat{U}_k = \left[MS_3^2 - \left(1 - ik\frac{\nu S_3^2}{S_2\, \bar{U}}\right) S_2^2\, \bar{U}^2 \right]^{-1} S_2 S_3 \bar{U}\, \hat{\Phi}_{sk} \quad .$$

6.4 Effect of the quasi-lagrangian semi-implicit scheme

In this case the total derivative is calculated using:

$$\frac{dX}{dt} = \frac{X^{t+\Delta t} - X_o^{t-\Delta t}}{2\Delta t} \quad ,$$

and the time averaging:

$$\bar{X}^{2t} = \frac{X^{t+\Delta t} + X_o^{t+\Delta t}}{2} \quad .$$

Applying this discretisation we finally obtain for the Fourier coefficients:

$$\hat{U}_k = \left[MS_3^2\, \mathcal{C}^2 - \left(1 - ik\frac{S_3^2 \nu e^{ik\bar{U}\Delta t}}{\frac{\mathcal{S}}{k\Delta t}}\right) \frac{\mathcal{S}^2}{k^2\, \Delta t^2} \right]^{-1} \frac{\mathcal{S}}{k\Delta t}\, \mathcal{C}\, S_3\, \hat{\Phi}_{sk} \quad .$$

with: $\mathcal{S} = \sin(k\bar{U}\,\Delta t)$ and: $\mathcal{C} = \cos(k\bar{U}\,\Delta t)$.

This relation shows that the stationary solution is modified by the time integration scheme. The greater the time step, the greater the modification.

7. NUMERICAL EXPERIMENTS WITH THE LINEAR BAROCLINIC MODEL

7.1 Characteristics of the linear model

We used a 47 point "Arakawa-C" grid with a 10 km mesh and cyclic boundary conditions (so that $X_1 = X_{46}$ and $X_2 = X_{47}$. The vertical discretisation was carried out by defining 30 σ levels equally spaced with respect to height (Δz = 600 m) in order to ensure an accurate representation of the vertical wave structures (Bougeault, 1987).

The orography was a "bell shaped" mountain defined by $h(x)=h_o(1+x^2/b^2)$ with h_o= 500 m and b= 25 km. The basic state was defined by the values $\bar{T}$ = 273°K, $\bar{p}_s$ = 1013.25 hPa and $\bar{U}$ = 20 ms^{-1}. The initial situation was calculated by adding to this basic state zero perturbations for T and U and $p_s = \bar{p}_s(e^{-gh(x)/R\bar{T}} - 1)$ for the surface pressure.

The model is then integrated up to 24 hours with various time-steps depending on the time integration scheme. The results of the integration of the linear model can be compared with the analytical solution (Figure 10), which was calculated by Bougeault (1987) after Klemp and Lilly (1978).

7.2 Explicit model

The explicit model has been integrated using a 10 s time-step up to 24 hours (Figure 11). The differences between the final state and the analytical solution are due to the unrealistic upper boundary condition $\dot{\sigma} = 0$ at $\sigma = 0$, which leads to a false reflection of the waves at the top of the atmosphere. As shown by Klemp and Lilly (1978), this drawback can be overturned by introducing a viscous dissipation layer (horizontal diffusion). The viscosity coefficient progressively grows from $\nu = 0$ at level $\sigma = 0.3$ to $\nu = 1.5 \times 10^5$ at level $\sigma = 0.15$ and aloft. The diffusive term is implicitly treated at the end of the time-step, in order to have an unconditionally stable scheme . The inclusion of this term in the momentum equation as well as in the thermodynamic equation allows to obtain a final state (Figure 11) which looks like the true solution we were looking for.

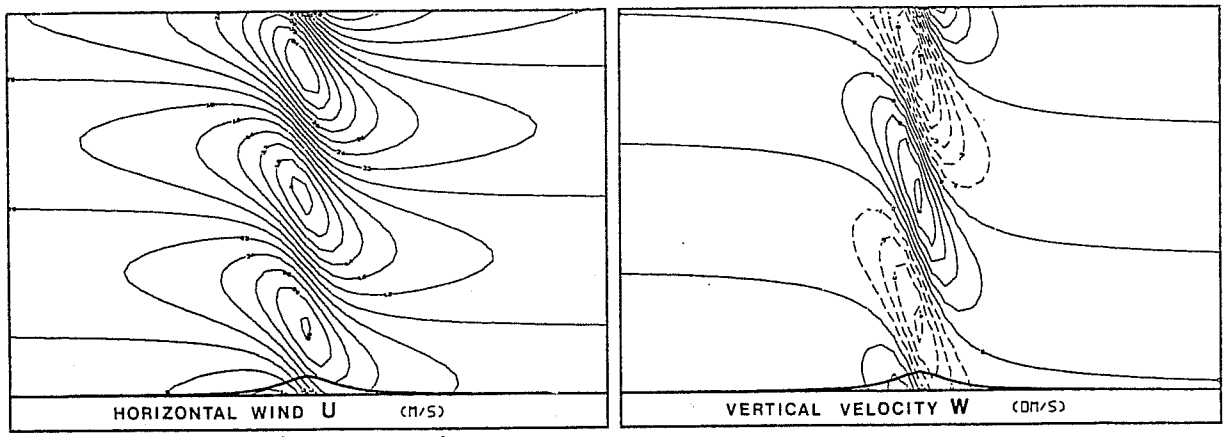

Figure 10. Analytical solution

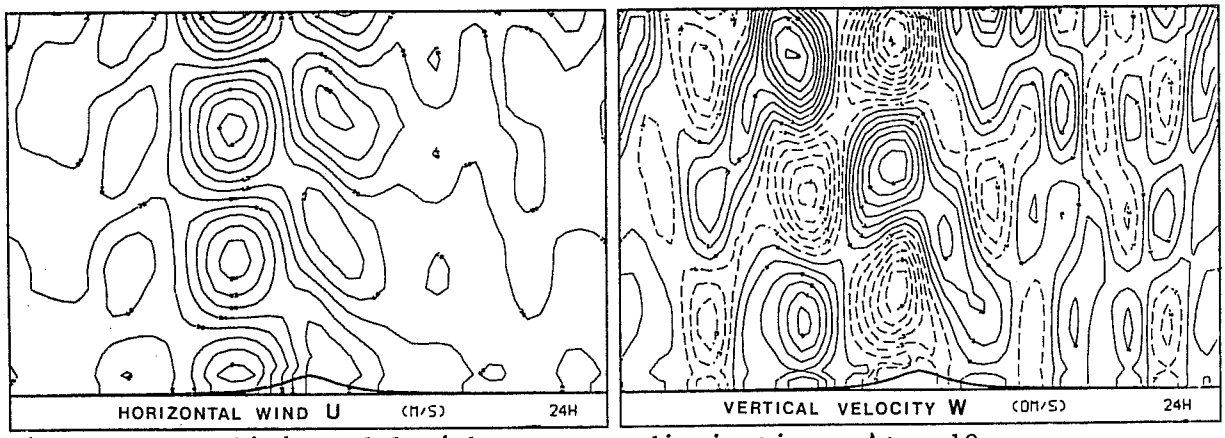

Figure 11. Explicit model without upper dissipation, Δt = 10 s

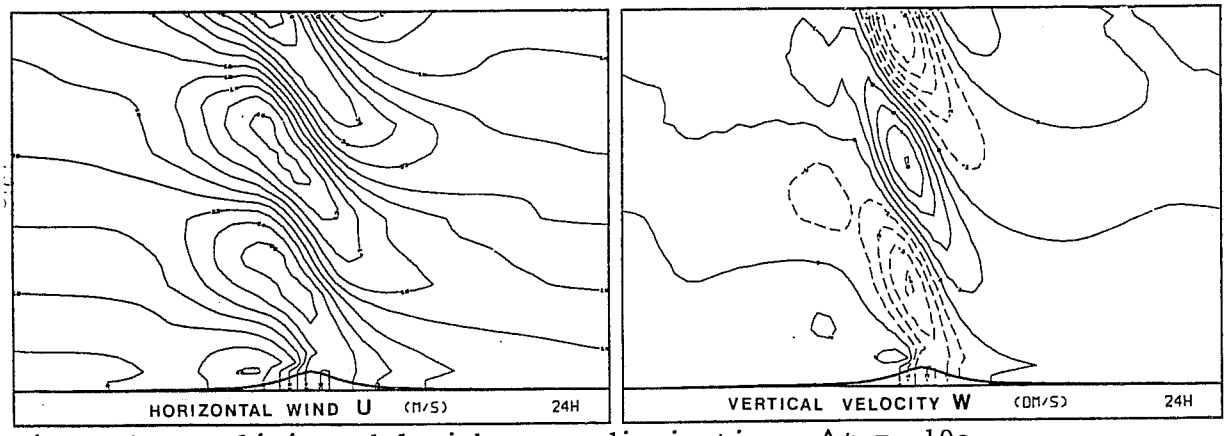

Figure 12. Explicit model with upper dissipation, Δt = 10s

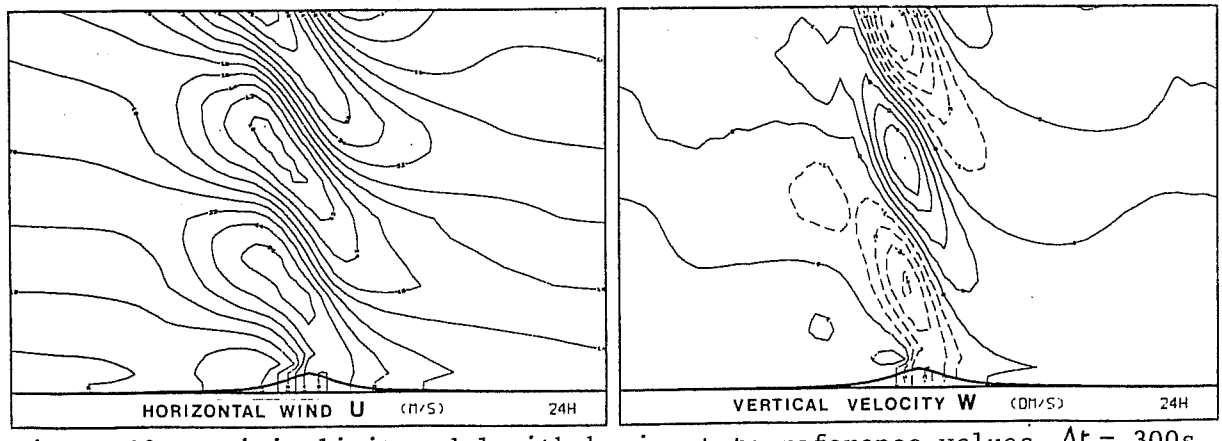

Figure 13. Semi-implicit model with basic state reference values, Δt = 300s

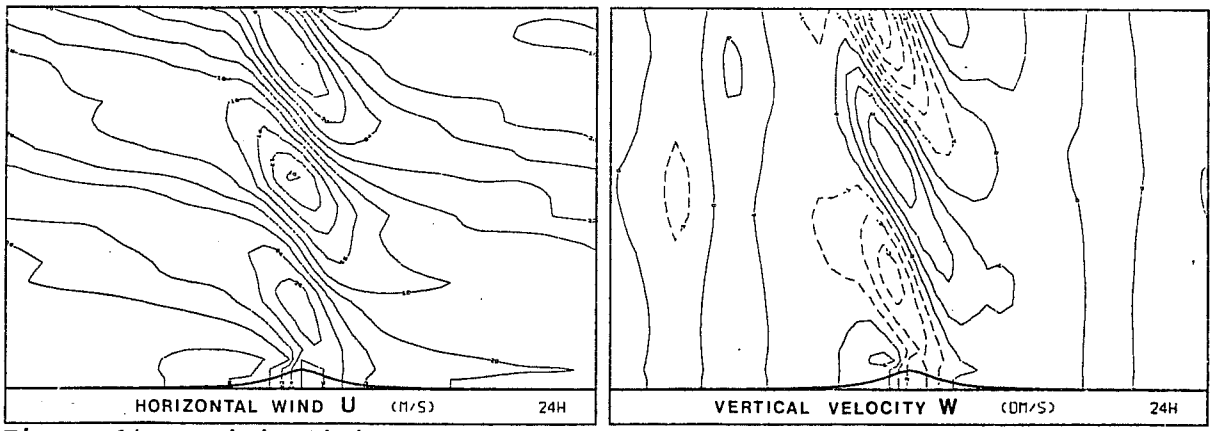

Figure 14. Semi-implicit model with modified reference values, Δt = 300s

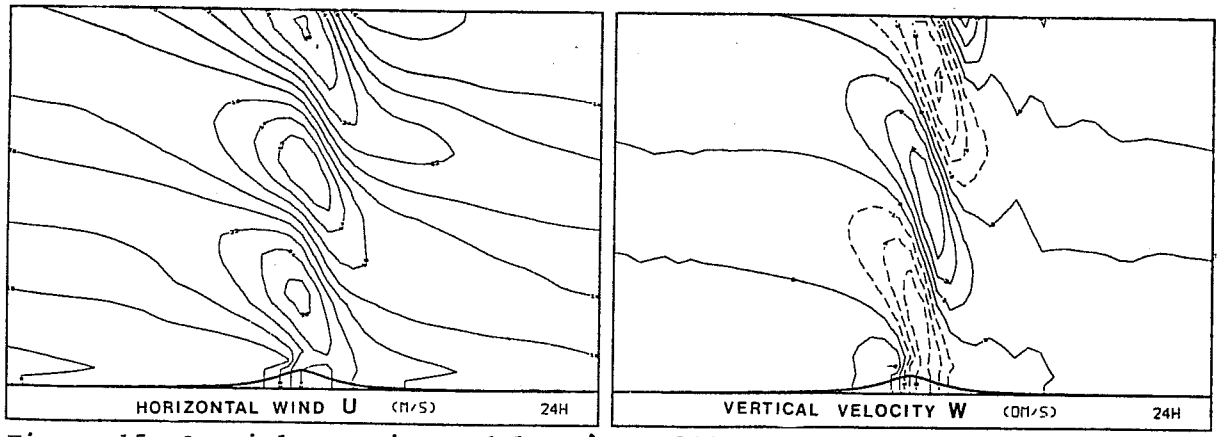

Figure 15. Quasi-lagrangian model, Δt = 300 s

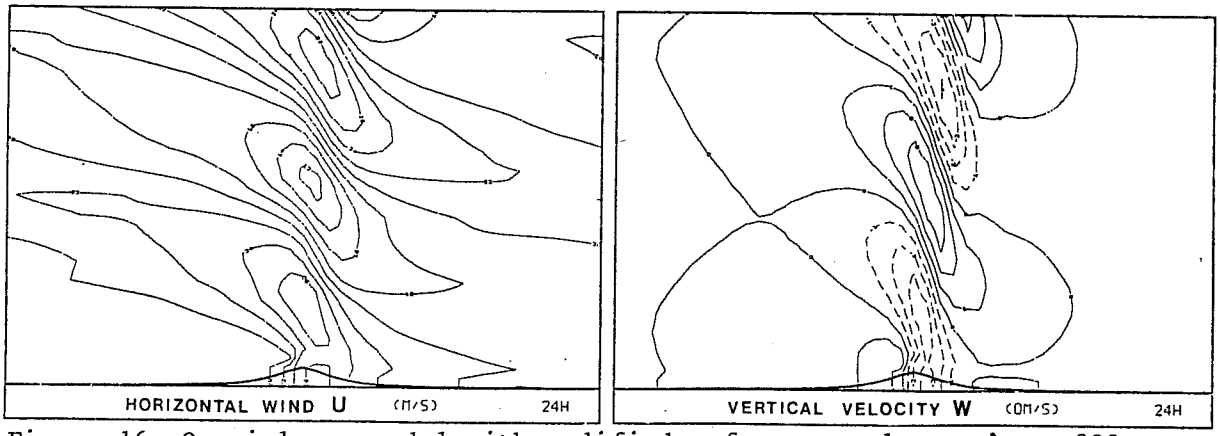

Figure 16. Quasi-lagr. model with modified reference values, Δt = 300s

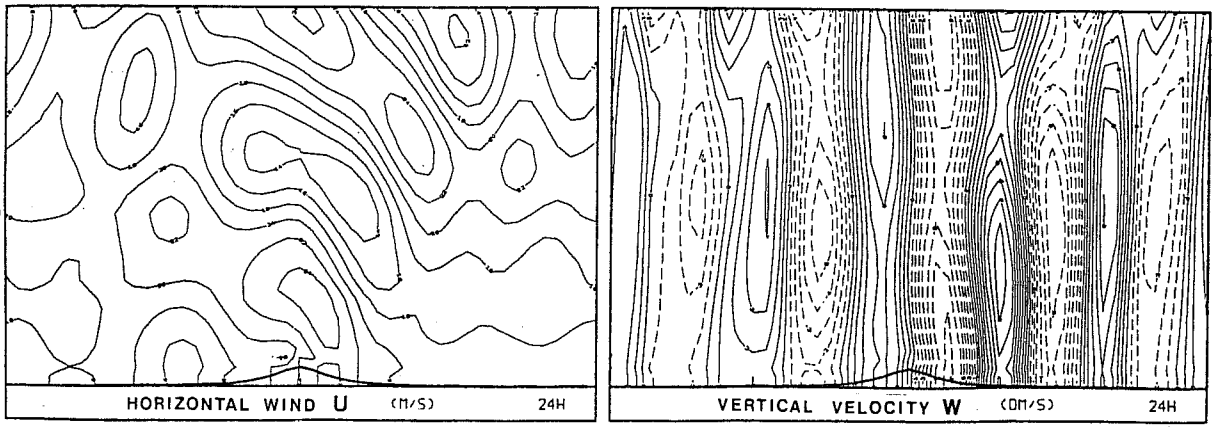

Figure 17. Quasi-lagrangian model with large time-step, Δt = 900 s

7.3 Semi-implicit model

The integrations are henceforth carried out with the upper dissipation terms. The semi-implicit model is characterized by an implicit treatment of the linear adaptative terms: they are calculated by using the same values as the basic state ones: ($\bar{T}$ = 273°K, $\bar{p}_s$ = 1013.25 hPa). Figure 13 shows the results, which have been obtained by using a 300 s time-step, and which are almost identical to the explicit ones. When evaluating the implicit part of the linear terms with different reference values ($\bar{T}$ = 290°K, $\bar{p}_s$ = 950 hPa) we have to explicitly compute the remaining linear terms but the final solution does not greatly differ from the preceding ones (Figure 14).

7.4 Quasi-lagrangian semi-implicit model

The quasi-lagrangian semi-implicit model using the Robert's method with linear intepolation at the origin point is at once integrated with a 300 s time-step. Two experiments have been carried out by using the same reference profiles as before. By looking at the results (Figures 15 and 16) we remark that they are slightly different from the semi-implicit ones (Figures 13 and 14). We observe a tilt of the line along the extrema of the vertical velocity.

By using a 900s time-step we obtain a final state (Figure 17) which is now dramatically different from the analytical one as it could be anticipated from calculations in Section 6.4.

7.5 Comparison with the computed stationary solution.

We calculated the stationary solution taking into account the effects of space as well as time discretisation. The relations we established in sections 6.3 and 6.4 for the Fourier components were transformed back into the physical space. Results given by explicit or semi-implicit method are plotted in figure 18 and exhibit a strong similarity with the results of the numerical integrations. Figures 19 and 20 show the reconstruction of the stationary quasi-lagrangian state by using time-steps of 300 s and 900 s respectively. The similarity between these figures (especially vertical velocities) and the results of the numerical integrations after 24 hours indicates that the odd behaviour of the model for large Courant numbers is due to the use of the quasi-lagrangian scheme.

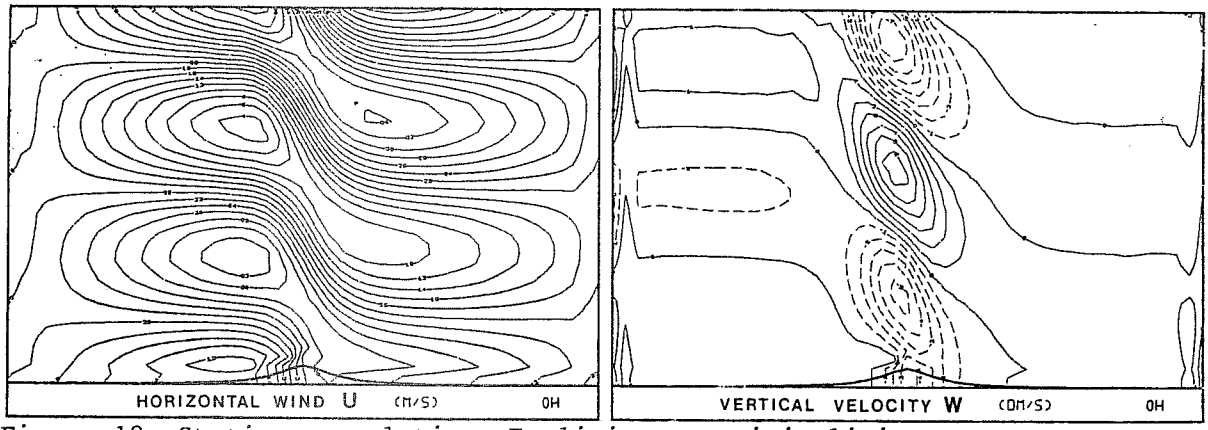

Figure 18. Stationary solution. Explicit or semi-implicit case

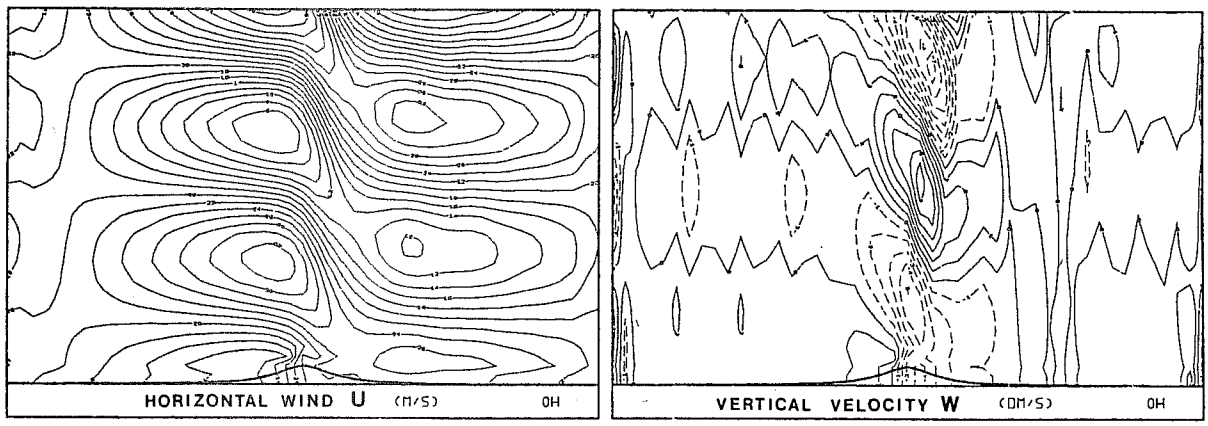

Figure 19. Stationary solution. Quasi-lagrangian case with $\Delta t = 300$ s

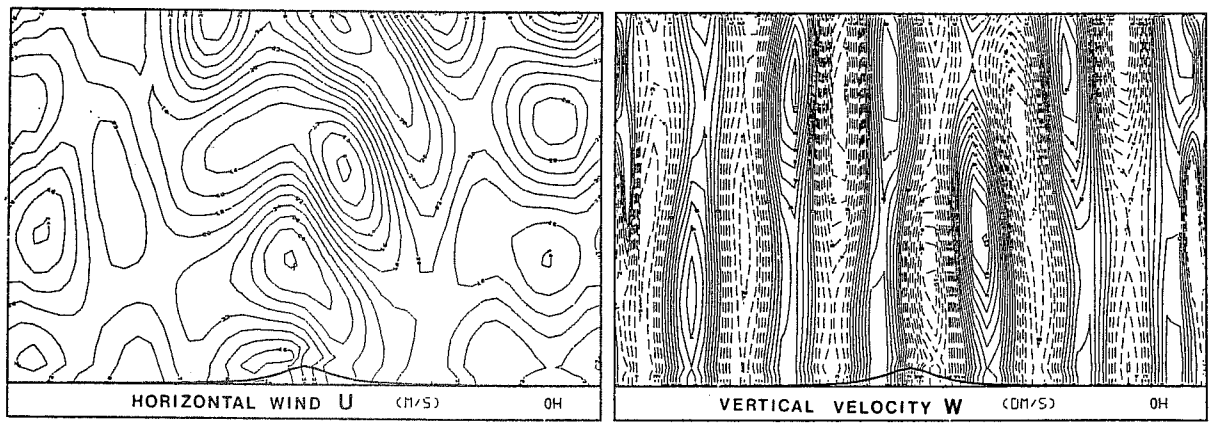

Figure 20. As fig. 19 except for $\Delta t = 900$ s

Common characteristics to figures 11 to 20:

Zonal winds (on the left) are in ms^{-1} and vertical velocities (on the right) in cms^{-1}. Contour interval are 4 ms^{-1} and 1 dms^{-1}, respectively. The vertical extension of the domain is limited to 10 000 m in these figures.

8. CONCLUSION

The effect of the quasi-lagrangian schemes has been investigated for two simplified two-dimensional models.

Calculations carried out with linear shallow water models show that the slow mode is rather well treated if the wavelength of the perturbation is large enough. These theoretical results are corroborated by numerical integrations using the non linear version of the model, which give good results even with Geleyn's method.

The study of the linear baroclinic equations show that the gravity wave velocities are strongly modified by the quasi-lagrangian scheme. In addition to that, it has been shown that this numerical scheme induces a wrong stationary solution; these results are also confirmed by numerical integrations of the linear model. Further investigations and tests of several variants of the method (horizontal as well as vertical quasi-lagrangian advection scheme, for example) have to be carried out in order to clarify our conclusions.

It would be premature to conclude that the quasi-lagrangian scheme could not be used for numerical weather prediction purposes. Several three-dimensional models using this kind of time integration have been succesfully implemented and the results have proven to be as good as the ones given by more classical models. It must also be pointed out that the baroclinic experiments presented correspond to an academic case where gravity waves dominate as is not the case for a large part of actual atmospheric flows. Nevertheless there is a suspicion that such schemes may not simulate well mesoscale circulations like flows forced by orography or events where the gravity waves play an important part.

References

Bates J.R., 1985. Semi-lagrangian advective schemes and their use in meteorological modelling. Lectures in Applied Mathematics Vol.22 , pp. 1-29.

Bougeault Ph., 1987. Etude de quelques écoulements orographiques à l'aide du modèle PERIDOT. Note de travail EERM N° 191, 85p.. Direction de la Météorologie Nationale, 77 Rue de Sèvres ,92106 Boulogne-Billancourt Cédex, France.

Geleyn J.F., 1986. Personal communication.

Imbard M., Joly A., Juvanon du Vachat R., 1986. Le modèle de prévision numérique PERIDOT. Formulation dynamique et modes de fonctionnement. Note de travail EERM n° 161, 70p. Direction de la Météorologie Nationale, 77 Rue de Sèvres, 92106 Boulogne-Bilancourt, Cédex, France.

Klemp J.B. and Lilly J.K, 1978. Numerical simulation of hydrostatic mountain waves. J. Atm. Sci. Vol. 35 pp. 78-107.

Ritchie H., 1986. Eliminating the interpolation associated with semi-lagrangian scheme. Mon. Wea. Rev. Vol 114. pp. 135-146.

Robert A.J., 1981. A stable numerical integration scheme for the primitive meteorological equations. Atmosphère-Océan Vol.19. pp. 35-46.

Robert A.J., 1982. A semi-lagrangian and semi-implicit numerical integration scheme for primitive meteorological equations. J. Met. Soc. Japan, Vol. 60. pp. 319-32